

White Matter Injury Induced by Perinatal Exposure to Glutaric Acid

Silvia Olivera-Bravo · Eugenia Isasi · Anabel Fernández · Juan Carlos Rosillo ·
Marcie Jiménez · Gabriela Casanova · María Noel Sarlabós · Luis Barbeito

Received: 23 September 2013 / Revised: 17 November 2013 / Accepted: 20 November 2013 / Published online: 3 December 2013
© Springer Science+Business Media New York 2013

Abstract Glutaric acid (GA) is a neurotoxic metabolite that accumulates in the CNS of patients with glutaric acidemia-I (GA-I), a neurometabolic disease caused by deficient activity of glutaryl-CoA dehydrogenase. Most GA-I patients display characteristic CNS lesions, mainly in the gray and white matter of basal ganglia and cerebral cortex. Neurons and astrocytes are believed to be vulnerable to millimolar concentrations of GA. However, little is known about the effects of GA on oligodendrocytes (OL) and the myelination process in the postnatal brain. Here, we show that a single intracerebroventricular administration of GA to rat neonatal pups induced a selective and long-lasting myelination failure in the striatum but no deleterious effect in the myelination of the corpus callosum. At 45 days post-GA injection, the myelinated area of striatal axonal bundles was decreased by 35 %, and the expression of myelin basic protein and myelin-associated glycoprotein (MAG) reduced by 25 and 60 %, respectively. This was accompanied by long lasting cytopathology features in MAG and

CC-1-expressing OLs, which was confirmed by transmission electron microscopy. Remarkably, GA did not induce acute loss of pre-OLs in the striatum as assessed by NG2 or PDGFR α immunohistochemistry, suggesting an indirect and progressive mechanism for OL damage. In accordance, GA-induced white matter injury was restricted to the striatum and associated to GA-induced astrocytosis and neuronal loss. In conclusion, the current evidence indicates a pathogenic mechanism by which GA can permanently affect myelin status.

Keywords Glutaric acidemia-I · Glutaric acid · Oligodendrocytes · Myelin

Introduction

Glutaric acidemia-I (GA-I) is a neurometabolic disease caused by deficiency of the mitochondrial enzyme glutaryl-CoA dehydrogenase (GCDH) involved in tryptophan, lysine, and hydroxy-lysine catabolism. Deficient GCDH activity results in the accumulation of neurotoxic concentrations of glutaric acid (GA) and related di-carboxylic metabolites (Goodman et al. 1975; Hoffmann et al. 1996). Most patients with GA-I develop characteristic encephalopathic crises in the childhood associated with irreversible striatal neurodegeneration clinically manifested by a variety of severe neurological symptoms (Strauss et al. 2003, 2007; Funk et al. 2005; Harting et al. 2009). Progressive cortical degeneration is also a common finding in GA-I. Some patients suffer chronically progressive neurological dysfunction without undergoing acute crises (Strauss et al. 2003, 2007; Harting et al. 2009). GA-I patients also develop white matter abnormalities, including variable degrees of leukoencephalopathy and/or periventricular

S. Olivera-Bravo · E. Isasi · M. Jiménez · M. N. Sarlabós
Neurobiología Celular y Molecular, IIBCE, Av. Italia 3318,
11600 Montevideo, Uruguay

A. Fernández · J. C. Rosillo
Neuroanatomía Comparada, IIBCE-Unidad Asociada a Facultad
de Ciencias, UdelaR, Av. Italia 3318, 11600 Montevideo,
Uruguay

M. Jiménez · G. Casanova
Unidad de Microscopía Electrónica, Facultad de Ciencias,
UdelaR, Iguá s/n, 11400 Montevideo, Uruguay

L. Barbeito (✉)
Institut Pasteur Montevideo, Mataojo s/n, 11400 Montevideo,
Uruguay
e-mail: barbeito@pasteur.edu.uy

white matter defects (Hoffmann et al. 1996; Kolker et al. 2002; Harting et al. 2009). Myelin alterations are the leading and almost exclusive pathological findings in cases of adult-onset GA-I (Kulkens et al. 2005; Gerstner et al. 2005; Harting et al. 2009), suggesting that white matter injury and neuronal loss may be independent pathophysiological processes in the disease.

The cellular and molecular mechanisms underlying GA-mediated toxicity in neonatal brain have been studied in different animal models of GA-I. The neurotoxic effects of GA and related metabolites in GA-I appear to be explained by excitotoxicity, disruption of mitochondrial energy homeostasis, and oxidative stress (for reviews, see Jafari et al. 2011; Wajner and Goodman 2011). However, GA-I accumulated metabolites fail to induce neuronal death in isolated cultured neurons (Freudenberg et al. 2004; Lund et al. 2004; Olivera-Bravo et al. 2011) or even in an *in vitro* model of rat organotypic brain cell cultures (Jafari et al. 2013), suggesting a complex mechanism involving disrupted intercellular crosstalk. The mouse model of GCDH deficiency that mimics the biochemical profiles of GA-I patients, exhibits marked diffuse spongiform myelinopathy without neuronal damage (Koeller et al. 2002, 2004), indicating the vulnerability of glial cells involved in myelin formation to GA-I accumulated metabolites.

We have developed an animal model of GA-I by injecting a single bolus of GA intracerebroventricularly (icv) to neonatal rat pups (Olivera et al. 2008; Olivera-Bravo et al. 2011). Treated pups respond to icv GA by transient convulsions resembling the encephalopathic crisis, and completely recovered with normal growth and no apparent motor sequels. In spite of the lack of symptoms, GA-injected pups develop abundant astrocytosis in the striatum followed by neuronal loss several weeks after GA administration (Olivera et al. 2008; Olivera-Bravo et al. 2011). In primary astrocytic cultures, GA also induces cell proliferation and a neurotoxic phenotype with the ability to kill striatal neurons through diffusible factors (Olivera-Bravo et al. 2011), further suggesting an indirect neurotoxic mechanism of GA mediated by astrocytes.

It is presently unknown whether GA can directly damage oligodendrocytes (OL) or its precursor cells leading to myelination defects, as well as the role played by concurrent astrogliosis. In this context, in the present study, we have used the icv GA administration model in newborn pups, to examine the effects of GA on postnatal myelination and the association with GA-induced astrocytosis.

Materials and Methods

Materials

GA, Sudan III, Luxol fast blue (LFB) reagents, diamino-2-phenylindole (DAPI), paraformaldehyde, and all other

chemicals of analytical grade were obtained from Sigma (St. Louis, MO). Fluoromyelin and secondary antibodies were from Molecular Probes (Eugene, OR). Primary antibodies were purchased to Molecular Probes, abcam (Cambridge, MA), and Millipore (Billerica, MA). Those that recognize GFAP and S100 β were from Sigma.

Animals and icv GA Administration

Experimental animal work was conducted using newborn Sprague–Dawley rats bred at the IIBCE animal facility. Animals were housed in cages with food and water *ad libitum* and maintained at controlled temperature and a 12 h light/dark cycle. Institutional guidelines according to national and international protection laws of vertebrate animals for scientific purposes were followed. All procedures were made to minimize animal pain or discomfort and approved by the corresponding ethical committees.

Five complete litters were used in this study. GA (2.5 μ mol/g body weight, pH 7.4) or vehicle (phosphate buffered saline (PBS), 10 mM, pH 7.4) was administered into the IV ventricle (Cisterna magna) between 12 and 24 h after birth. Each pup received up to 5 μ l injected by using a 30G needle attached to a Tygon tube extension to allow correct manipulation. After the icv injection, animals were allowed to recover at 30 °C during 15–30 min and returned to the mother until weaning at 21 postnatal days or processing for tissue analysis.

After 1, 12, 21, and 45 days post-injection (DPI), animals were anesthetized with 90:10 mg/kg ketamine/xilazine and intracardially perfused with 4 or 10 % paraformaldehyde (PAF) in 10 mM, pH 7.4, PBS. After fixation, brains were quickly removed, maintained overnight at 4 °C in the corresponding fixative and then changed to PBS until sectioning. A 1000S Leica (Buffalo Grove, IL) vibratome was used to obtain 30–50- μ m thick consecutive coronal series containing the striatal region. Sections were stored either free-floating at 4 °C or mounted on gelatin-coated slides until analyzed.

Myelin Histochemistry

Coronal brain sections containing the corpus callosum and the striatal region were permeabilized with 0.3 % Triton-PBS during 20 min, immersed in 70 % ethanol for 2 min, and then incubated with 2 % Sudan III for 30 min at room temperature. The reaction was stopped with 70 % ethanol and then with distilled water. Stained sections were stuck to glass slides, left drying at room temperature, and mounted in glycerol, to be further imaged. Microphotographs of the corpus callosum and striatal regions were obtained in a BX61 Olympus (Center Valley, PA) direct microscope attached to a DP70 Olympus camera. The

Image J (NIH, Bethesda, MD) software was used to measure the net intensity (mean gray value minus the background) and the size of Sudan III-stained regions in different experimental conditions. The ratio of net intensities was calculated as the coefficient between the averaged intensity shown by GA-injected animals and that shown by their respective age-matched controls. The ratio of sizes of areas was obtained by dividing the total Sudan III positive striatal area of GA-injected animals between the total Sudan III positive striatal areas of controls. At least, 12–15 slices were measured according to the age of the animals studied.

One every five sections containing the striatum were stained with LFB (Sheehan and Hrapchak 1980). Briefly, sections were incubated overnight at 60 °C in 0.1 % LFB, sequentially rinsed in 95, 70, and 30 % ethanol and distilled water. Differentiation was made with 0.1 % lithium carbonate and completed with 70 % ethanol, rinsed in water, and finally incubated with 0.05 % cresyl violet for 2 min. Stained sections were de-hydrated with increasing ethanol concentrations, acetone, and xylene and mounted with DPX for further light microscopy analysis.

Other 3–5 brain sections containing the striatum of all conditions were directly stained at room temperature with 100 µl of a 1:300 dilution of the stock solution of green Fluoromyelin during 20 min. Sections were rinsed, mounted in glycerol, and imaged in a confocal FV300 Olympus microscope using a 488 nm laser. Size of striatal areas positive to LFB and Fluoromyelin was measured and related to respective controls as mentioned above.

Immunohistochemistry

For each animal and staining procedure, 5–7 equivalent sections covering the striatum were analyzed. Anatomical landmarks (aspect, size and position of the anterior commissures, corpus callosum, lateral ventricles, striatum, and nucleus accumbens; Paxinos and Watson 2007) were used to ensure that parameters were analyzed at similar levels within and between groups.

Immunohistochemistry against myelin basic protein (MBP), myelin-associated glycoprotein (MAG), APC product gene (CC-1 protein), neuroglycan 2 (NG2), and the receptor alpha for platelet derived growth factor (PDGFR α) was used to recognize myelin or myelin-associated proteins, mature OL, and pre-oligodendrocytes, respectively. A monoclonal anti-S100 β antibody was used to identify striatal astrocytes. All the assays were performed on free-floating sections that were washed, permeabilized 20 min with 0.1–0.3 % Triton X-100, and incubated 30 min in blocking buffer (PBS containing 0.3 % Triton X-100 and 5 % bovine serum albumin). Afterward, a 4 °C overnight incubation was performed with one or two of the following

antibodies: anti-MBP or anti-MAG (1:250, Molecular Probes), anti-NG2 (1:300, Millipore); anti-PDGFR α (1:300, Millipore), anti-APC product gene (1:300, abcam), anti-S100 β (1:500, Sigma). Then sections were rinsed and incubated 90 min with 1:800 dilutions of 1 mg/mL secondary antibodies conjugated to fluorescent probes (Molecular Probes). After three washes, samples were mounted in glycerol containing 1 µg/mL DAPI. As negative controls, the primary or secondary antibodies were omitted.

2048 × 2048 images were obtained in a FV300 Olympus confocal microscope provided with 405, 488, 546, and 633 nm lasers. Microphotographs of representative areas were taken with all acquisition parameters identical for control and GA-treated animals (PMT below to 650 V, 0 % gain, 0 V offset, and at maximum pixel size). In some cases, z-stacks were performed maintaining same parameters and thickness in all conditions. Once pictures were obtained, cells positive to DAPI and each specific marker were counted in 5–7 fields of each striatal section. 15–21 slices from 5 to 7 animals per condition were analyzed at equivalent striatal levels.

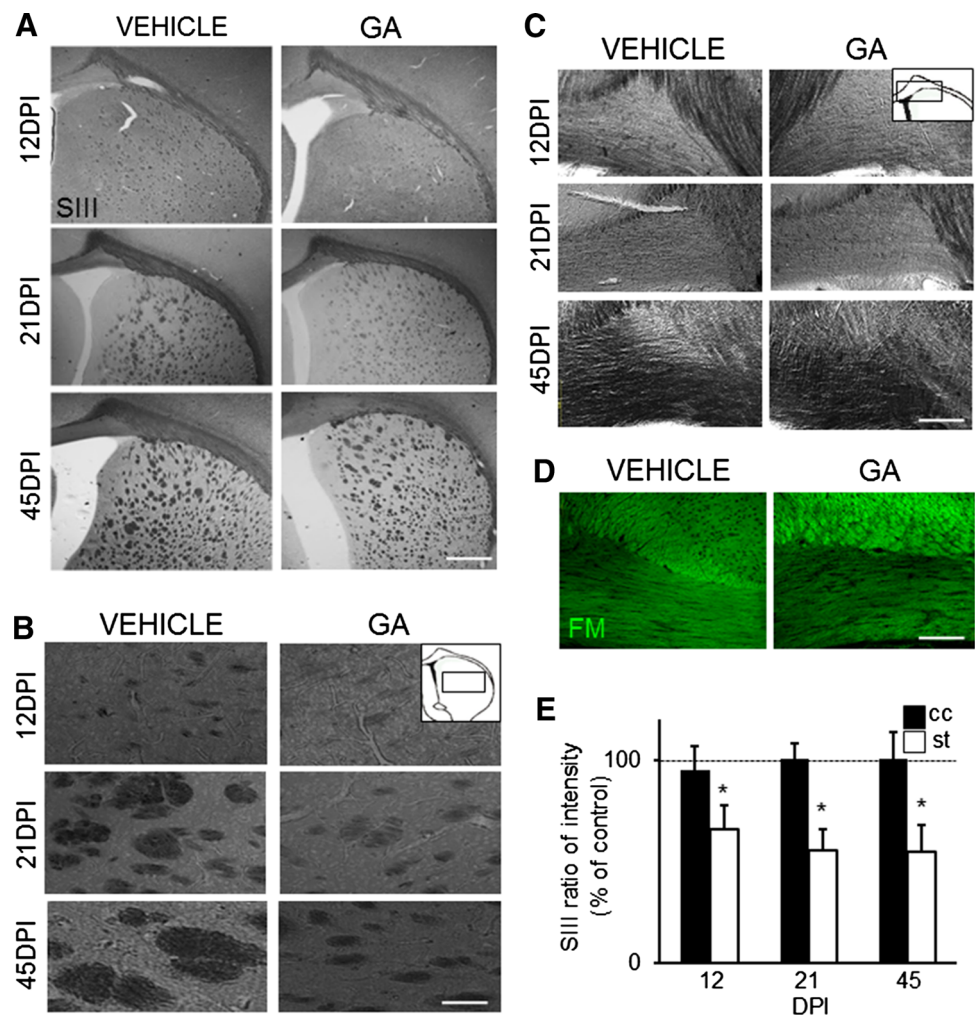
Analysis of PDGFR α Expression by Western Blotting Analysis

To assess the expression of the pre-oligodendrocyte marker PDGFR α 24 h after GA administration, three different batches of striatal samples each one obtained by pooling tree rat pups injected with vehicle (controls) or with GA were processed for Western blotting analysis. Briefly, fresh samples were collected in tissue lysis buffer, homogenized, and protein quantitated. Denatured samples were seeded, and a typical SDS-PAGE electrophoresis was run (Díaz-Amarilla et al. 2011). Proteins were transferred to PVDF membranes that were further incubated with a 1:1,000 dilution of anti-PDGFR α antibody (Millipore), or with a 1:4,000 dilution of anti- β actin antibody (Sigma) that was used as a protein loading control. Both antibodies were developed with Pierce ECL kit (Rockford, IL) and bands analyzed with the Image J gel analyzer tool.

Transmission Electron Microscopy (TEM) Analysis

Five animals per condition and age were processed for TEM imaging and analysis. After being anesthetized animals were intracardially perfused with 4 % PAF plus 2.5 % electron microscopy grade glutaraldehyde (Sigma). Brains were quickly dissected and immersed 120 min in the same fixative solution. Each region containing the striatum was separated as a single 400 µm slice that was further cut at 40 nm thick. Ultrathin sections were post-fixed with 1 % osmium tetroxide, contrasted with saturated

Fig. 1 Effect of icv GA on myelination of striatal and corpus callosum axons. Panoramic (a) and higher magnification (b) images of Sudan III histochemistry of transversal brain sections showing positive myelinated areas at 12, 21, and 45 days after icv GA administration (DPI) evidencing long-term decrease in the striatum of GA pups related to age-matched controls. The inset shows the area analyzed. Calibration bars = 200 and 60 μm for (a) and (b), respectively. c Corpus callosum Sudan III positive staining evidencing preserved myelination at all ages analyzed. Scheme shows the area analyzed, that is close to the cingulum. Calibration bar = 60 μm . d Fluoromyelin staining showing that GA-animal preserved corpus callosum fibers at 45DPI. Calibration bar = 30 μm . e Quantitation of the intensity of SIII positive signals in corpus callosum (cc) and striatum (st) from 5 to 7 GA-injected animals as compared to 5–7 controls denoting significant differences only in the striatum (* $p < 0.05$). Data are the mean \pm SD



solutions of uranyl acetate and lead citrate and then imaged in a TEM JEOL JEM 1010 microscope operating at 80 kV. Pictures were taken with a Hamamatsu C-4741-95 photonic camera.

Statistical Analysis

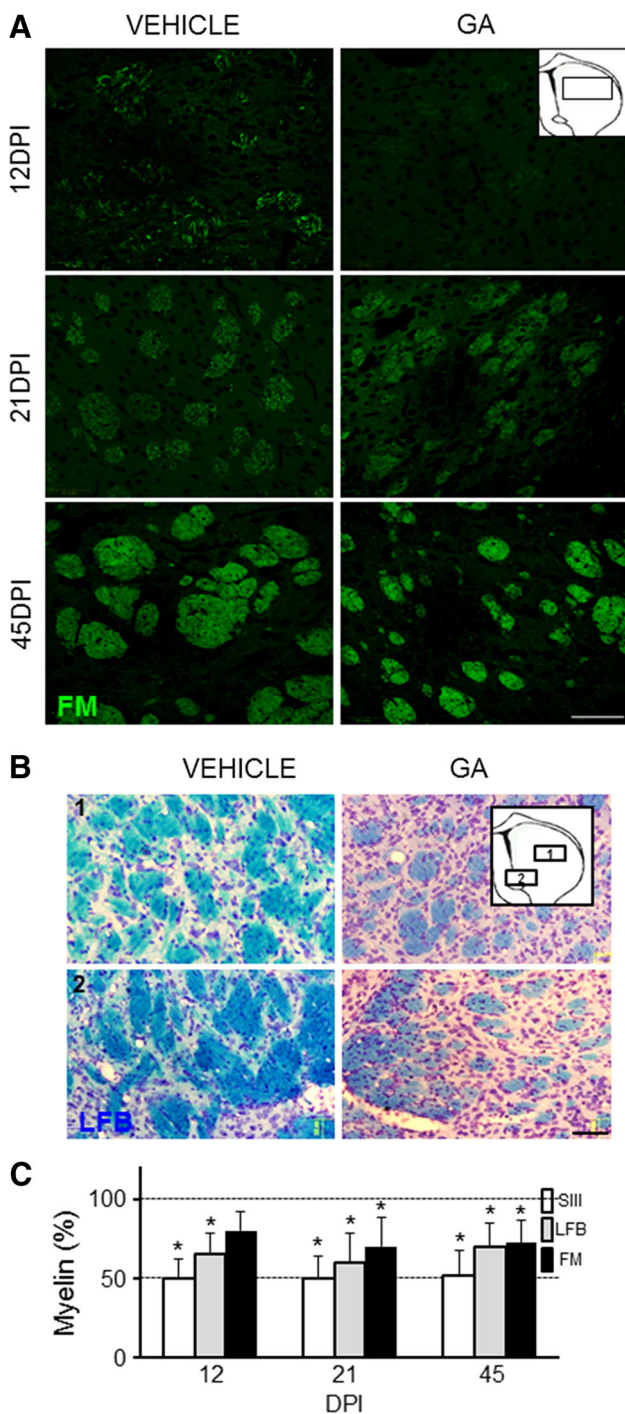
Data analysis was performed with Sigma Stat 2.0. Cell numbers, and myelinated areas were studied by means of one-way ANOVA followed by Tukey or Tukey–Kramer post hoc analysis if necessary. All results are presented as mean \pm SD; $p \leq 0.05$ was considered significant.

Results

Myelination Failure Induced by icv GA Administration to Rat Pups

Rat pups were injected at postnatal day 0 with a single bolus of 2.5 $\mu\text{mol/g}$ body weight GA into the cisterna

magna. This treatment induced tonic–clonic convulsions that lasted up to 15 min after injection and were followed by 20–30 min hypotonic phases (Olivera et al. 2008; Olivera-Bravo et al. 2011). 80 % of the rats injected with GA survived without showing any gross difference regarding to the age-matched controls. The analysis of postnatal myelination was performed in the striatum and corpus callosum at 12, 21, and 45 days post-injection (DPI). GA-injected animals showed ~50 % decreased content in striatal myelin through 12DPI to 45DPI compared to respective controls (Fig. 1a, b). As myelination progressed with age, myelin-positive areas associated with axonal bundles in GA-injected pups were smaller and more condensed than controls (Fig. 1b). In contrast, myelination in the corpus callosum was unaffected by GA administration at all ages (Fig. 1c, e). When myelinated areas were stained with the more sensitive probe Fluoromyelin, the GA-induced reduction of myelinated areas oscillated between 25 and 30 % through 12DPI to 45DPI, with respect to controls (Fig. 2). The probe also evidenced the



fragmentation and compaction of axonal bundles at 45DPI (Fig. 2a). Altered myelinated areas in GA-animals were also confirmed by the fragmentation and fading of the LFB turquoise lipid staining (Fig. 2b). The comparative quantitation made at all ages and with all markers confirmed significant GA-induced myelination failure in the striatum (Fig. 2c).

◀ **Fig. 2** Long lasting striatal myelination failures upon perinatal GA administration. **a** Fluoromyelin staining of striatal axonal packages showing decreased intensity of labeling at 12 and 21DPI and a fragmentation and condensation of axonal packages in GA-animals at 45DPI. **b** Luxol fast blue staining of striatal bundles at 45DPI evidencing decreased lipidic myelinated areas as suggested by fading turquoise staining in GA-injected animals. *Insets* show the areas analyzed. Calibration bars = 50 and 100 μ m for (a) and (b), respectively. **c** Quantitation of the size of striatal-myelinated areas in 7 GA-injected animals as compared to 7 age-matched controls evaluated after staining with Sudan III (SIII), Luxol fast blue (LFB), and Fluoromyelin (FM). Note the long-term reduction at all ages and with all markers employed. Data are the mean \pm SD indicates statistical significance at $*p < 0.05$

Decreased Expression of Striatal Myelin-Associated Proteins Upon GA Administration

The analysis of myelin and myelin-associated proteins was performed in the striatum. In control animals, myelin basic protein (MBP) staining progressively increased with age, delineating the whole volume of striatal axonal packages by 45DPI (Fig. 3a). In comparison, the progression of MBP expression in GA-injected animals was 20–35 % lower than in controls (Fig. 3a, c). In the case of MAG, it showed less expression that MBP in controls at all ages (Fig. 3b), and then a more dramatically decrease in GA-injected pups along the age (Fig. 3c).

GA-Induced Oligodendrocyte Pathology in the Striatum

The effect of GA on the number and morphology of OL was assessed by using antibodies that recognize MAG and adenomatosis polyposis coli (APC) gene product (clone CC1), the latter being expressed in the cell body of mature OL (Bhat et al. 1996). CC1-positive OLs exhibited profound cytopathological features in GA-animals, as suggested by swollen appearance and shorter processes (Fig. 4a). In addition, the number of CC-1 cells progressively decrease after GA administration, being ~50 % of control numbers at 45DPI (Fig. 4a). In control animals, the perimeter of OL bodies was selectively stained with MAG antibody, which is consistent with the protein delivery and arrangement around axons (Fig. 4b). In comparison, MAG staining in GA-animals was apparently decreased in the distal processes and more accumulated in the cell body (Fig. 4b).

TEM of 12 DPI striatal sections evidenced that most OLs from GA-injected animals exhibited features of cell damage including swelling of nuclear membrane and dilated ER cisternae (Fig. 5a). When compared to controls, it was also evident a slight increase of myelin sheaths with

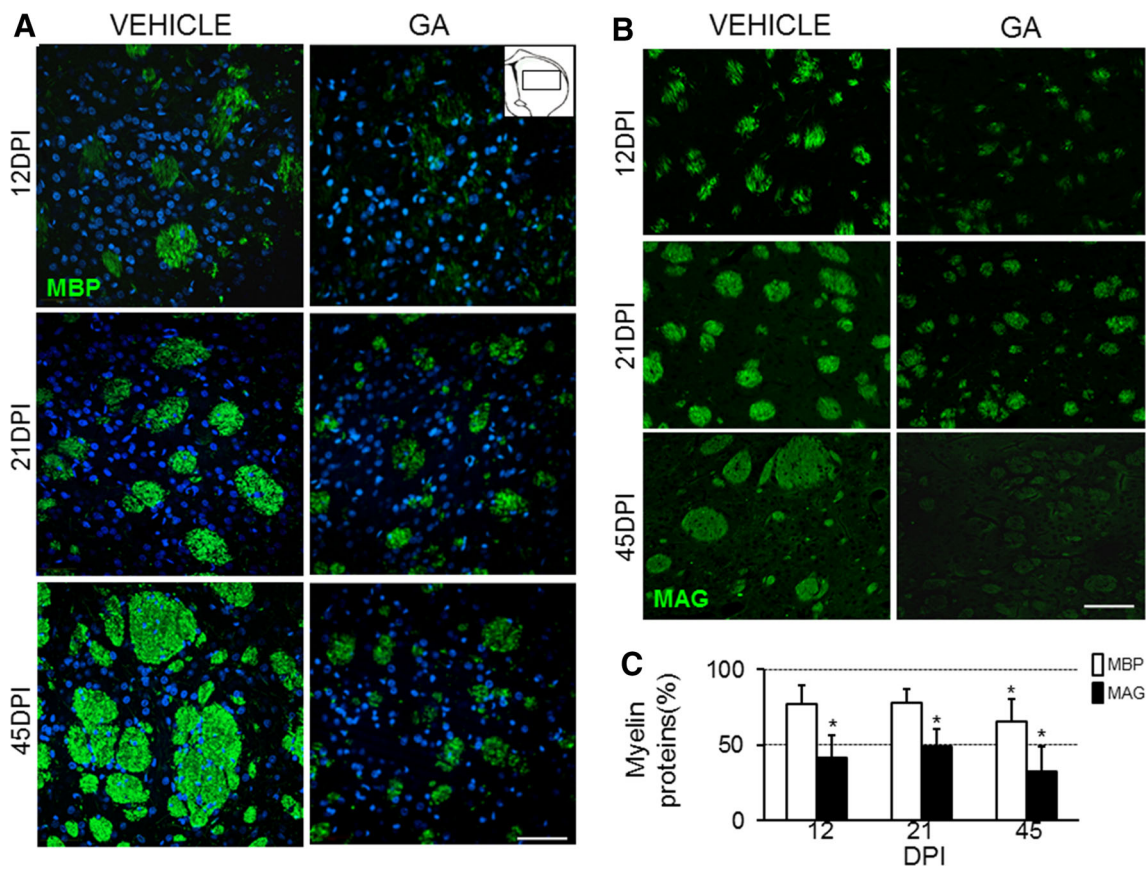


Fig. 3 Icv GA causes altered expression of myelin-associated proteins. **a** Typical pattern of myelin basic protein (MBP) immunoreactivity in 5–7 GA-injected animals evidencing decreased levels in striatal axonal bundles as well as fragmentation at all ages analyzed when compared to controls. Blue staining of nuclei was made with DAPI. Calibration bar = 50 μ m. *Insert* shows the area imaged.

b Myelin-associated glycoprotein (MAG) immunostaining showing a progressively decreased signal in the axonal bundles in GA-injected animals as compared to controls. Calibration bar = 50 μ m. **c** Quantitation of MBP and MAG immunoreactive areas in 5–7 GA-injected animals as compared to 5–7 age-matched controls. Data are the mean \pm SD; statistical significance was taken at $*p < 0.05$

abnormal folding or altered compaction (Fig. 5b). Axons from GA-injected pups appeared more vacuolated and exhibited a slight decrease in the internal diameter as well as in the ratio among internal and external diameters, which is comparable to the *g* ratio. In comparison, axons in control animals displayed regular round shapes and complete myelin wraps with preserved periodicity as expected for normal myelination stages (Mori and Leblond 1970).

GA-Induced Myelin Failure is not Associated to Acute Toxicity to PreOLs but to Astrocytosis

To analyze whether myelination failure in the striatum was associated to acute effects on OL precursor cells, the striatal population of OL progenitors was analyzed 24 h after GA administration. No changes in morphology were found in both controls and GA-animals. NG2 cells appeared as isolated small cells displaying tiny spiny process in a 3D-like arrangement. PDGFR α -stained delicate small cells that are located around axonal bundles and bear sparse smooth

processes (Fig. 6a). GA did not modify PDGFR α protein levels when compared to controls (Fig. 6b), neither the number of preOLs (Fig. 6c). In comparison to controls, in GA-animals, the number of astrocytes stained with S100 β increased by twofold (Fig. 6c), and cells appeared hypertrophic (Fig. 6d), both highly suggestive of acute dysfunctional astrocytosis.

Discussion

In the present study, we found that a transient increase in GA levels in the CNS triggers a long lasting perinatal white matter injury that resembles the hypomyelination observed in patients with GA-I (Bahr et al. 2002; Kolker et al. 2002; Funk et al. 2005). GA-induced myelination failure was not observed in the corpus callosum but restricted to the basal ganglia; brain areas that are most vulnerable to follow degeneration in patients with GA-I (Goodman et al. 1975; Strauss et al. 2003, 2007; Funk et al. 2005). On the other

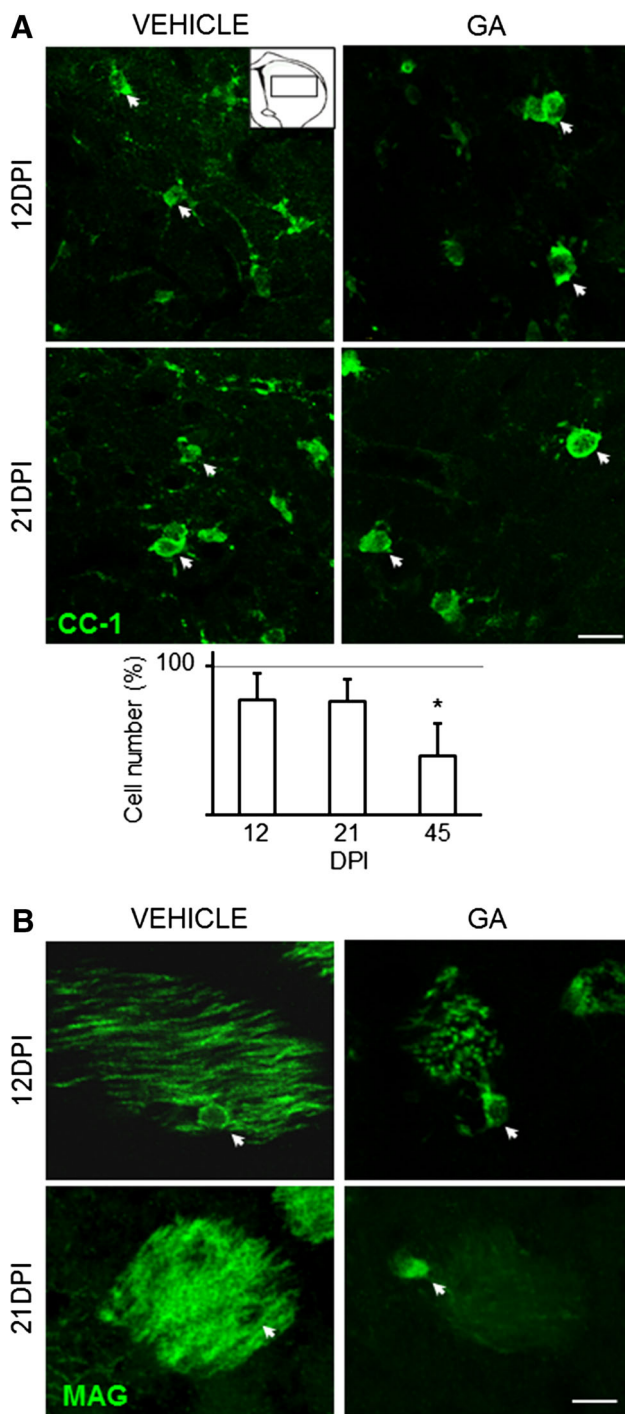


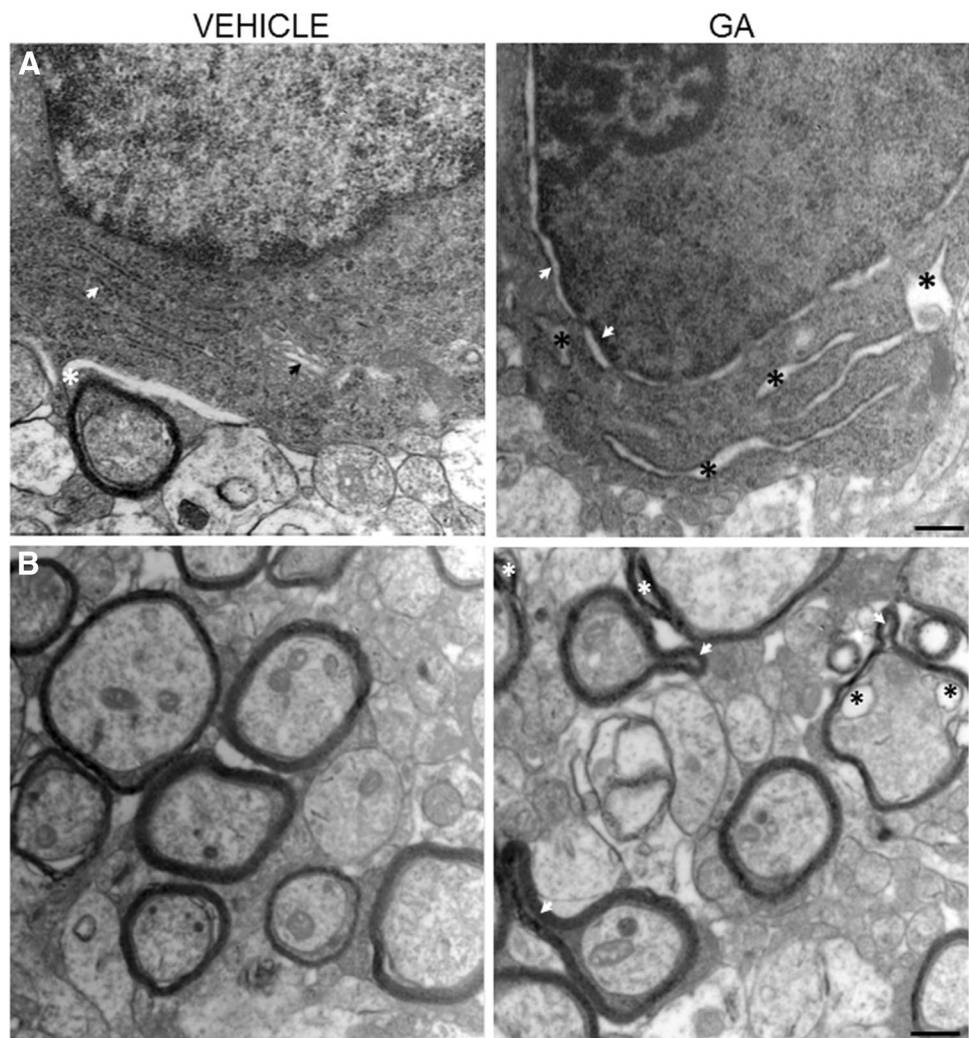
Fig. 4 Effects of GA administration on oligodendrocytes **(a)** 8 μm Z-stacks of sections stained with APC gene product (CC-1) antibody showing apparent swelling of the cell body and disappearance of cell processes in oligodendrocytes from GA-animals at 12 and 21 DPI (white arrows) as compared to controls. The scheme shows that the area analyzed, and the chart indicates the number of striatal APC gene product positive cells in GA-animals related to age-matched controls. Data are the mean \pm SD means $*p < 0.05$. **b** MAG immunofluorescence of 12 μm Z-stacks of striatal axonal bundles at high magnification to show OL bodies (white arrows). Calibration = 15 and 20 μm , for **(a)** and **(b)**, respectively. Seven animals were used in each condition

hand, GA did not induce acute damage to OL precursors in neonatal pups, the OL cytopathology being delayed by several days following the single exposure to GA, suggesting an indirect neurotoxic mechanism. Such delayed toxicity compares to the delayed loss of striatal neurons induced by icv GA (Olivera-Bravo et al. 2011), which is mediated at least in part, by reactive and hypertrophic astrocytes responsive to GA. Therefore, the GA-induced neurotoxicity appears to require a complex cellular interplay that after an initial triggering elicited by toxic levels of GA, auto-perpetuate during weeks leading to the progressive damage of neurons and myelinating OLs.

Our icv GA injection model seems to reproduce at least in part the encephalopathic crisis as well as the striatal neuronal loss and myelination defects observed in GA-I patients. In comparison, the paradigmatic knock-out GCDH mouse model of the disease expected to reproduce the human disease (Koeller et al. 2002, 2004), does not develop neuronal loss despite having high levels of GA-I accumulated metabolites. Zinnanti et al. (2006, 2007) reported that a high lysine diet dramatically increased GA-I metabolites in 4- and 8-week old GCDH KO mice and caused neuronal death. However, these results have not been reproduced in another study (Seminotti et al. 2012), suggesting that increased levels of GA-I metabolites do not systematically lead to neuronal death, and that other local or systemic factors are needed to trigger neurodegeneration. Remarkably, a marked diffuse spongiform myelinopathy is the most common neuropathological finding in GCDH deficient mice (Koeller et al. 2002, 2004), and it is also present in those mice submitted to a high lysine diet (Zinnanti et al. 2006, 2007) further indicating the vulnerability of glial cells to GA-I metabolites. These findings may explain the white matter compromise in GA-I patients, including those with the late-onset variant (Bahr et al. 2002; Kolker et al. 2002).

Myelination failure induced by GA administration was evidenced by several myelin markers and become significant by postnatal day 12, when striatal myelination is still incipient (Downes and Mullins 2013). Icv GA administration induced a progressive and major decrease in MBP immunoreactivity from axonal bundles. MBPs are integral components of the CNS myelin that contribute to myelin formation, development, and stability (for a review see Harauz and Boggs 2013). In addition, the full-length, early-developmental 21.5-kDa splice isoform promotes OL differentiation (Baron et al. 2000), whereas the 18.5-kDa adult predominating form contributes to cytoskeleton assembly, mediation of signaling pathways, and maintenance of calcium and cell homeostasis (Harauz and Boggs 2013). As the antibody employed recognized all MBP isoforms, the observed decrease in MBP is in accordance with the ultrastructural OL cytopathology evidenced by TEM.

Fig. 5 Ultrastructural pathology of oligodendrocytes and myelin in GA-injected animals. **a** A TEM microphotograph from a representative control pup, showing one OL displaying the characteristic continuity between the nuclear envelope and the cytoplasm, and a well-organized ER (*white arrow*), Golgi apparatus (*black arrow*). The *white asterisk* shows a mesaxon wrapping an axon. The OLs from GA-injected animals on the *right* show a prominent separation between the nuclear membrane and the cytoplasm (*white arrows*), and a disorganized ER with dilated cisternae (*black asterisks*). **b** TEM images showing normal myelinated axons in controls at 12DPI. GA-injected animals presented *smaller axons* of anomalous shapes with abundant myelin outfolding (*white asterisks*), abnormal misfolding (*white arrows*), and vacuoles (*black asterisks*). Five animals were studied in each condition. Calibration bars = 500 nm



In GA-injected animals, MAG levels progressively decreased until its virtual disappearance from axonal bundles at 45DPI. MAG is one of the most abundant myelin-associated proteins of the central OL surface (Pernet et al. 2008), implicated in the organization of the axonal cytoskeleton by regulating neurofilament spacing and phosphorylation, and the caliber of myelinated axons (Yin et al. 1998). Altered MAG levels have been associated to delayed myelination and disturbed ultrastructure of myelin (Li et al. 1994; Montag et al. 1994). Taken together, the long lasting deleterious effects of the single GA administration in myelin-associated proteins indicate a permanent OL pathology. It is uncertain whether these defects are cause or consequence of myelination failure.

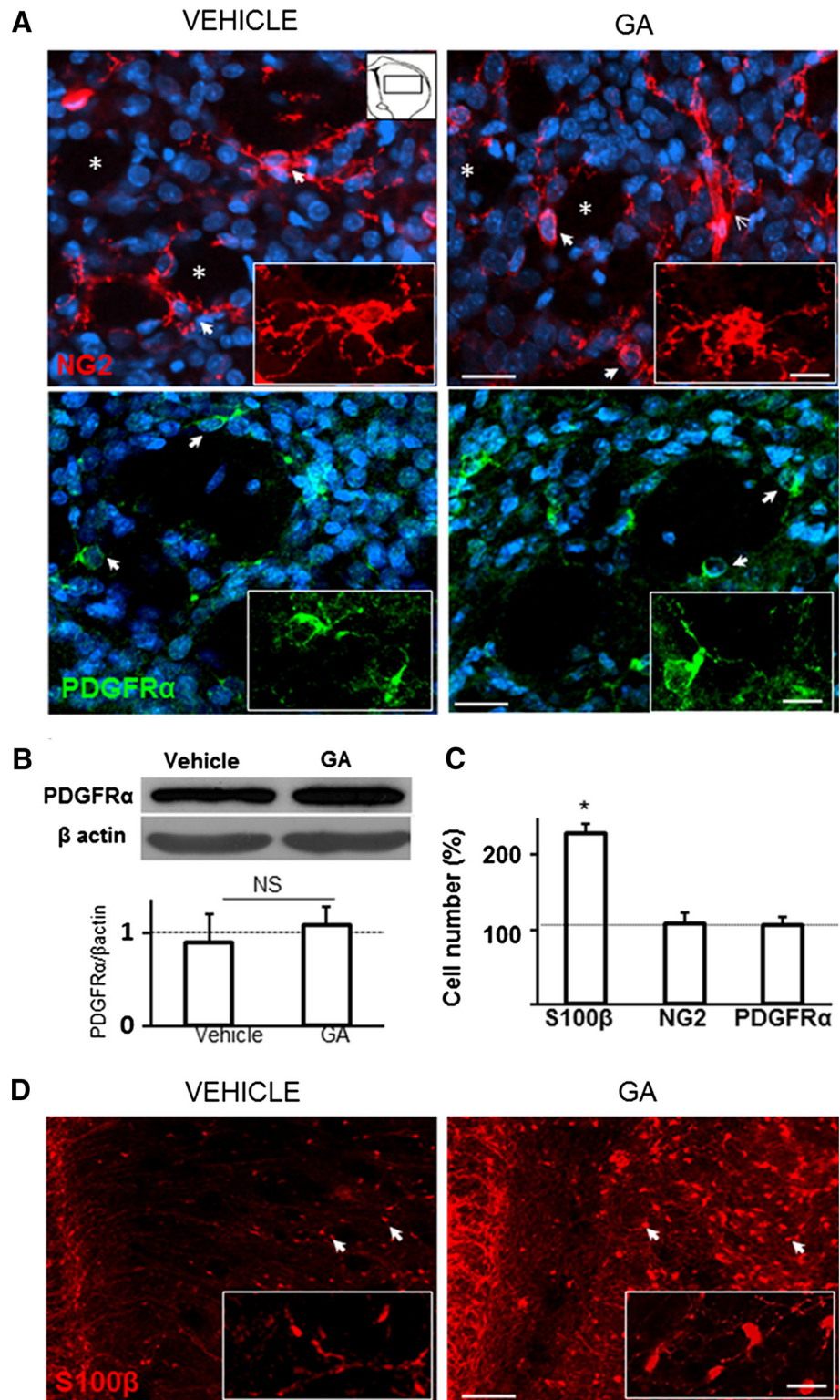
Accordingly, GA-injected animals showed significant morphological alterations in OL bodies early during myelination onset and then a further decrease in the number of CC-1 expressing mature OLs. TEM analysis revealed smaller axons, myelin misfolding and several OL cytopathological features including ER swelling. These data

suggest that GA administration creates a cellular environment that promotes chronic OLs pathology possibly including ER stress and altered protein trafficking (Bauer et al. 2002), which anticipates altered OL-axonal interactions.

The mechanisms by which astrocyte dysfunction can lead to myelination failure remain unknown. It has been shown that multiple trophic factors are required for the survival of developing OLs; many of them are produced by astrocytes (Barres et al. 1993; Nash et al. 2011). Because OL precursor survival is dependent on astrocyte trophic support (Barres et al. 1993; Nash et al. 2011), even small changes in astrocytic function may be detrimental to oligodendrocyte maturation and survival. Evidence also indicates that reactive astrocytes occurring in pathological conditions can lead to defective myelination (De Keyser et al. 2008; Nash et al. 2011; Verkhatsky et al. 2012). Neonatal astrocyte damage in Alexander disease (Liem and Messing 2009; Verkhatsky et al. 2012) or periventricular leukomalacia (Dean et al. 2011) has been implicated in the

Fig. 6 Acute effects of icv GA on preOLs and astrocytes.

a NG2 and PDGFR α staining in the striatum of control (vehicle) and GA-injected rats assessed 24 h after GA administration evidencing lack of significant effect of GA on preOL number and morphology. DAPI nuclear staining showed the preservation of typical striatal cell arrangement around axonal packages (*white asterisks*). *Insets* show morphological details at higher magnification. Calibration bars = 30 and 10 μ m for pictures and *insets*, respectively. **b** Western blotting and PDGFR α / β actin ratio showing no changes in PDGFR α expression in 20 μ g of striatal tissue obtained 24 h after GA administration when compared to controls. NS means nonstatistical significance. **c** Quantitation of the number of striatal S100 β , NG2, and PDGFR α positive cells related to controls. Note the increase in S100 β astrocytic population. Pictures are representative of data obtained in seven animals per experimental group. Data are the mean \pm SD * p < 0.05. **d** Panoramic view of S100 β striatal immunoreactivity evidencing a dramatic increase in both the number and size (*arrows*) of S100 β positive cells in GA-injected animals. *Insets* show the increased cell body, and the appearance of protruding cell processes in GA-animals when comparing to controls. Calibration = 100 and 50 μ m for images and *insets*, respectively



triggering of CNS pathologies leading to myelination failure. Therefore, myelin deficit in GA-I may be caused by early astrocytic dysfunction elicited by GA and related metabolites. Astrocytes are preferentially vulnerable to GA because they can actively uptake the di-carboxylic acid

(Olivera et al. 2008; Magni et al. 2009; Lamp et al. 2011), which lead to mitochondria dysfunction and increased proliferation. GA causes astrocytes to develop a poorly differentiated phenotype with high S100 β and low GFAP expression (Olivera et al. 2008; Olivera-Bravo et al. 2011).

Such inability of astrocytes to reach appropriate differentiation may critically compromise their support to neurons and OL differentiation.

In conclusion, the present study describes a new animal model to induce localized myelination failure in postnatal development, associated to astrocytosis and neuronal loss. Our results may explain clinical observations of some GA-I patients, where white matter defects continue to aggravate after normalization of metabolic parameters by dietary managements (Zinnanti et al. 2007). Therapies targeting astrocytes and OLs may prevent and/or revert myelination failure and permanent neurological deficits in GA-I.

Acknowledgments All authors declare no conflict of interest. This work was funded by the Uruguayan Program for the Development of Technology (PDT) [76/23], and PEDECIBA Biología.

References

- Bahr O, Mader I, Zschocke J, Dichgans J, Schulz JB (2002) Adult onset glutaric aciduria type I presenting with a leukoencephalopathy. *Neurology* 59(11):1802–1804
- Baron W, de Jonge JC, de Vries H, Hoekstra D (2000) Perturbation of myelination by activation of distinct signaling pathways: an in vitro study in a myelinating culture derived from fetal rat brain. *J Neurosci Res* 59(1):74–85
- Barres BA, Schmid R, Sendtner M, Raff MC (1993) Multiple extracellular signals are required for long-term oligodendrocyte survival. *Development* 118(1):283–295
- Bauer J, Bradl M, Klein M, Leisser M, Deckwerth TL, Wekerle H, Lassmann H (2002) Endoplasmic reticulum stress in PLP-overexpressing transgenic rats: gray matter oligodendrocytes are more vulnerable than white matter oligodendrocytes. *J Neuropathol Exp Neurol* 61:12–22
- Bhat RV, Axt KJ, Fosnaugh JS, Smith KJ, Johnson KA, Hill DE, Kinzler KW, Baraban JM (1996) Expression of the APC tumor suppressor protein in oligodendroglia. *Glia* 17(2):169–174
- De Keyser J, Mostert JP, Koch MW (2008) Dysfunctional astrocytes as key players in the pathogenesis of central nervous system disorders. *J Neurol Sci* 267:3–16
- Dean JM, Riddle A, Maire J, Hansen KD, Preston M, Barnes AP, Sherman LS, Back SA (2011) An organotypic slice culture model of chronic white matter injury with maturation arrest of oligodendrocyte progenitors. *Mol Neurodegener* 6:46–55
- Díaz-Amarilla P, Olivera-Bravo S, Trias E, Cragolini A, Martínez-Palma L, Cassina P, Beckman J, Barbeito L (2011) Phenotypically aberrant astrocytes that promote motoneuron damage in a model of inherited amyotrophic lateral sclerosis. *Proc Natl Acad Sci USA* 108(44):18126–18131
- Downes N, Mullins P (2013) The development of myelin in the brain of the juvenile rat. *Toxicol Pathol*. doi:10.1177/0192623313503518
- Freudenberg F, Lukacs Z, Ullrich K (2004) 3-Hydroxyglutaric acid fails to affect the viability of primary neuronal rat cells. *Neurobiol Dis* 16(3):581–584
- Funk CB, Prasad AN, Frosk P, Sauer S, Kolker S, Greenberg CR, Del Bigio MR (2005) Neuropathological, biochemical and molecular findings in a glutaric acidemia type I cohort. *Brain* 128:711–722
- Gerstner B, Gratopp A, Marcinkowski M, Siffringer M, Obladen M, Bühner C (2005) Glutaric acid and its metabolites cause apoptosis in immature oligodendrocytes: a novel mechanism of white matter degeneration in glutaryl-CoA dehydrogenase deficiency. *Pediatr Res* 57:771–776
- Goodman SI, Markey SP, Moe PG, Miles BS, Teng CC (1975) Glutaric aciduria: a “new” disorder of amino acid metabolism. *Biochem Med* 12(1):12–21
- Harauz G, Boggs JM (2013) Myelin management by the 18.5 and 21.5 kDa classic myelin basic protein isoforms. *J Neurochem* 125(3):334–361
- Harting I, Neumaier-Probst E, Seitz A, Maier EM, Assmann B, Baric I, Troncoso M, Mühlhausen C, Zschocke J, Boy NP, Hoffmann GF, Garbade SF, Kölker S (2009) Dynamic changes of striatal and extrastriatal abnormalities in glutaric aciduria type I. *Brain* 132:1764–1782
- Hoffmann GF, Athanassopoulos S, Burlina AB, Duran M, de Klerk JB, Lehnert W, Leonard JV, Monavari AA, Muller E, Muntau AC, Naughten ER, Plecko-Starting B, Superti-Furga A, Zschocke J, Christensen E (1996) Clinical course, early diagnosis, treatment, and prevention of disease in glutaryl-CoA dehydrogenase deficiency. *Neuropediatrics* 27:115–123
- Jafari P, Braissant O, Bonafé L, Ballhausen D (2011) The unsolved puzzle of neuropathogenesis in glutaric aciduria type I. *Mol Genet Metab* 104(4):425–437
- Jafari P, Braissant O, Zavadakova P, Henry H, Bonafé L, Ballhausen D (2013) Ammonium accumulation and cell death in a rat 3D brain cell model of glutaric aciduria type I. *PLoS One* 8(1):e53735
- Koeller DM, Woontner M, Crnic LS, Kleinschmidt-DeMasters B, Stephens J, Hunt EL, Goodman SI (2002) Biochemical, pathologic and behavioral analysis of a mouse model of glutaric acidemia type I. *Hum Mol Genet* 11:347–357
- Koeller DM, Sauer S, Wajner M, de Mello CF, Goodman SI, Woontner M, Mühlhausen C, Okun JG, Kolker S (2004) Animal models for glutaryl-CoA dehydrogenase deficiency. *J Inher Metab Dis* 27:813–818
- Kolker S, Mayatepek E, Hoffmann GF (2002) White matter disease in cerebral organic acid disorders: clinical implications and suggested pathomechanisms. *Neuropediatrics* 33(5):225–231
- Kulkens S, Harting I, Sauer S, Zschocke J, Hoffmann GF, Gruber S, Bodamer OA, Kölker S (2005) Late-onset neurologic disease in glutaryl-CoA dehydrogenase deficiency. *Neurology* 64:2142–2144
- Lamp J, Keyser B, Koeller DM, Ullrich K, Bräulke T, Mühlhausen C (2011) Glutaric aciduria type 1 metabolites impair the succinate transport from astrocytic to neuronal cells. *J Biol Chem* 286:17777–17784
- Li C, Tropak MB, Gerlai R, Clapoff S, Abramow-Newerly W, Trapp B, Peterson A, Roder J (1994) Myelination in the absence of myelin-associated glycoprotein. *Nature* 369:747–755
- Liem RK, Messing A (2009) Dysfunctions of neuronal and glial intermediate filaments in disease. *J Clin Invest* 119:1814–1824
- Lund TM, Christensen E, Kristensen AS, Schousboe A, Lund AM (2004) On the neurotoxicity of glutaric, 3-hydroxyglutaric, and trans-glutaconic acids in glutaric acidemia type 1. *J Neurosci Res* 77(1):143–147
- Magni DV, Furian AF, Oliveira MS, Souza MA, Lunardi F, Ferreira J, Mello CF, Royes LF, Figuera MR (2009) Kinetic characterization of 1-[(3)H]glutamate uptake inhibition and increase oxidative damage induced by glutaric acid in striatal synaptosomes of rats. *Int J Dev Neurosci* 27:65–72
- Montag D, Giese KP, Bartsch U, Martini R, Lang Y, Blüthmann H, Karthigasan J, Kirschner DA, Wintergerst ES, Nave KA, Zielasek J, Toyka KV, Lipp HP, Schachner M (1994) Mice deficient for the myelin-associated glycoprotein show subtle abnormalities in myelin. *Neuron* 13:229–246
- Mori S, Leblond CP (1970) Electron microscopic identification of three classes of oligodendrocytes and a preliminary study of their proliferative activity in the corpus callosum of young rats. *J Comp Neurol* 139:1–28

- Nash B, Thomson CE, Linington C, Arthur AT, McClure JD, McBride MW, Barnett SC (2011) Functional duality of astrocytes in myelination. *J Neurosci* 31:13028–31308
- Olivera S, Fernández A, Latini A, Rosillo JC, Casanova G, Wajner M, Cassina P, Barbeito L (2008) Astrocytic proliferation and mitochondrial dysfunction induced by accumulated glutaric acidemia I (GAI) metabolites: possible implications for GAI pathogenesis. *Neurobiol Dis* 32:528–534
- Olivera-Bravo S, Fernández A, Sarlabós MN, Rosillo JC, Casanova G, Jiménez M, Barbeito L (2011) Neonatal astrocyte damage is sufficient to trigger progressive striatal degeneration in a rat model of glutaric acidemia-I. *PLoS One* 6:e20831–e20840
- Paxinos G, Watson C (2007) *The rat brain in stereotaxic coordinates*. Academic Press, Sydney
- Pernet V, Joly S, Christ F, Dimou L, Schwab ME (2008) Nogo-A and myelin-associated glycoprotein differently regulate oligodendrocyte maturation and myelin formation. *J Neurosci* 28:7435–7444
- Seminotti B, Amaral AU, da Rosa MS, Fernandes CG, Leipnitz G, Olivera-Bravo S, Barbeito L, Ribeiro CA, de Souza DO, Woontner M, Goodman SI, Koeller DM, Wajner M (2012) Disruption of brain redox homeostasis in glutaryl-CoA dehydrogenase deficient mice treated with high dietary lysine supplementation. *Mol Genet Metab* 108(1):30–39
- Sheehan D, Hrapchak B (1980) *Theory and practice of histotechnology*, 2nd edn. Battelle Press, Columbus
- Strauss KA, Puffenberger EG, Robinson DL, Morton DH (2003) Type I glutaric aciduria, part 1: natural history of 77 patients. *Am J Med Genet C Semin Med Genet* 121C:38–52
- Strauss KA, Lazovic J, Wintermark M, Morton DH (2007) Multimodal imaging of striatal degeneration in Amish patients with glutaryl-CoA dehydrogenase deficiency. *Brain* 130(Pt 7):1905–1920
- Verkhatsky A, Sofroniew MV, Messing A, deLanerolle NC, Rempel D, Rodriguez JJ, Nedergaard M (2012) Neurological diseases as primary gliopathies: a reassessment of neurocentrism. *ASN Neuro* 4:e00082–e00100
- Wajner M, Goodman SI (2011) Disruption of mitochondrial homeostasis in organic acidurias: insights from human and animal studies. *J Bioenerg Biomembr* 43(1):31–38
- Yin X, Crawford TO, Griffin JW, Tu P, Lee M, Li C, Roder J, Trapp BD (1998) Myelin-associated glycoprotein is a myelin signal that modulates the caliber of myelinated axons. *J Neurosci* 18:1953–1962
- Zinnanti WJ, Lazovic J, Wolpert EB, Antonetti DA, Smith MB, Connor JR, Woontner M, Goodman SI, Cheng KC (2006) A diet-induced mouse model for glutaric aciduria type I. *Brain* 129(Pt 4):899–910
- Zinnanti WJ, Lazovic J, Housman C, LaNoue K, O'Callaghan JP, Simpson I, Woontner M, Goodman SI, Connor JR, Jacobs RE, Cheng KC (2007) Mechanism of age-dependent susceptibility and novel treatment strategy in glutaric acidemia type I. *J Clin Invest* 117:3258–3270